PNAS

Supporting Information for

Redefining the human corneal immune compartment using dynamic intravital imaging.

Laura E Downie,[a,1,2✉*] Xin Yuan Zhang,[a] Mengliang Wu,[a] Senuri Karunaratne,[a] Joon Keit Loi,[b] Kirthana Senthil,[a,b] Sana Arshad,[c] Kirstie Bertram,[c] Anthony Cunningham,[c] Nicole Carnt,[c,d,e] Scott N Mueller,[b,1,2✉] Holly R Chinnery[a,1,2✉]

[a]Department of Optometry and Vision Sciences, The University of Melbourne, Carlton, Victoria, Australia; [b]Department of Microbiology and Immunology, The University of Melbourne, The Peter Doherty Institute for Infection and Immunity, Melbourne, Australia. [c]The Westmead Institute for Medical Research, The University of Sydney, Sydney, Australia; [d]School of Optometry and Vision Science, UNSW, Kensington, Australia; [e]Institute of Ophthalmology, University College London, London, United Kingdom.

[1]L.E.D., S.N.M. and H.R.C. jointly supervised this work.

[✉2]To whom correspondence may be addressed. Email: ldownie@unimelb.edu.au; smue@unimelb.edu.au; holly.chinnery@unimelb.edu.au

This PDF file includes:

Supplementary information for materials and methods
Figures S1-S4
Table S1-S3
Legends for Movies S1 to S8

Other supporting materials for this manuscript include the following:

Movies S1 to S8

Supplementary Information Materials and Methods

Human Participants. Participant testing involved questions to confirm demographic information, and general and ocular health status. Allergy symptoms were quantified using the Eye Allergy Patient Impact Questionnaire.

Eligible participants were 18 to 40 years inclusive, in good general health with no self-reported conditions affecting eye health (other than seasonal allergy), not pregnant or breastfeeding, had not previously undergone ocular surgery, did not have a history of contact lens wear and had not

received a vaccination for COVID-19 or influenza within two weeks of enrolment. Potential participants with a history of ocular infection or inflammation, dry eye disease(1), or with corneal abnormalities (including histories of ocular injury, keratoconus and corneal dystrophies) were excluded.

Individuals in the untreated allergy group were required to have not used an antihistamine medication within one week of enrolment, or a corticosteroid or immunomodulatory agent within one month of enrolment. Participants for the CL study comprised a subpopulation (n=4) of healthy controls (naïve to CL wear, per the eligibility criteria) who re-attended on a separate day for baseline Fun-IVCM imaging (pre-CL), with repeat imaging after approximately three hours of wearing a soft silicone-hydrogel contact lens (Air Optix Aqua, Alcon, USA).

IVCM Imaging. For IVCM image acquisition, illumination was set at automatic brightness for all images. The region of interest was captured by having the contralateral (left) eye focus on a fixation target. Repeated volume scans of this same corneal region were acquired every four to seven minutes for 20 to 40 minutes. Sequence scans at the level of the basal epithelium were acquired at the corneal apex to quantify additional cell density parameters. The central sampling area involved analyzing 12 high-quality non-overlapping IVCM images per participant, to provide cell density calculations within 30% of the anticipated true mean, 95% of the time(2). Per our protocols, IVCM images that were blurred, had an inconsistent imaging depth, or showed vignetting were removed from all potential analysis sets (3, 4). No post-capture image enhancements were performed.

Analysis of immune cell dynamics and macrophage morphology. For each parameter, the mean value across the capture period was used as the representative value per cell, normalized per unit of time (minute) where appropriate. Individual cell tracks were manually determined using the 'Manual Tracking' function in Image J. Cell track parameters (*x-y* coordinates for the cell centroid, and the inter-frame time interval) were exported as CSV files, to derive cell instantaneous speed, displacement speed, meandering index, outreach ratio, arrest coefficient and the linearity of forward progression (see Table S2). All cells that could be reliably followed and had tracks with a minimum of four timepoints were incorporated in the analyses. To quantify DC dSEARCH (dendrite surveillance extension and retraction cycling habitude)(5), the absolute values of the changes in dendrite length for all dendrites over the capture period was summed to derive the dSEARCH index and normalized per minute (normalized dSEARCH index).

Stromal macrophages exhibit amoeboid-like cytoplasmic ruffling movements. To identify and quantify macrophage density in the stroma, 2D time-lapsed videos were curated to visualize dynamic cells compared to stationary keratocytes. For each timepoint, volume scans were used to create z-stacks (typically two to four layers, depending on focal plane consistency) from the anterior-most stromal layers. Matched *x-y* regions were extracted from each timepoint and used to create a new stack, which was then registered using the Linear Stack Alignment with SIFT-affine function in FIJI. Hyperstacks were created for 2D visualization of the time-dependent behaviors of stromal cells. Morphometric parameters (i.e., field area, cell area, perimeter, roundness, circularity and solidity; see Table 2) were calculated. To demonstrate the dynamic behaviors of macrophages compared to keratocytes, the co-efficient of variation (based on cell area) was calculated across all timepoints; masks were generated to portray the total area occupied by a selection of representative cells over time.

Human corneal tissue immunohistochemistry. After washing the corneal tissue in (PBS) three times, small pieces of corneal flat mounts were permeabilized in PBS containing 1% triton for 2 hours, then blocked in PBS containing 3% bovine serum albumin and 0.1% triton for 45 minutes. Corneal tissues were then incubated overnight (4C) in blocking solutions containing primary antibodies mouse anti-human CD45 (BD Pharmingen, Cat No. 555480, 1:250 dilution), followed by 3 washes with PBS and incubation with secondary antibody goat anti-mouse 488 (Jackson Immunoresearch, Cat No. 115-547-003). After 3 washes in PBS (10 minutes each), tissues were

incubated in mouse anti-human CD3 PE 594 (BD Pharmingen, Cat No. 562280, 1:200) and Hoechst (Sigma-Aldrich, MO, USA, Cat No. 14533, 1:500) for two hours at room temperature. After three final washes in PBS, tissues were cover-slipped, epithelium facing up.

Human corneal tissue processing for flow cytometry. Corneal samples from each donor eye were placed into a dispase solution (0.02 mg/mL dispase (neutral protease, Worthington Industries, Columbus, OH, USA), 1:100 gentamicin (Sigma-Aldrich) in RPMI 1640 (Lonza, Switzerland) per sample) and incubated overnight at 4°C. Samples were placed in a water bath for 37°C for 15 minutes and then vortexed to allow cells from the epithelium to slough off. Using a slit angled knife, remaining epithelium of the sample was scraped and suspended in the dispase solution. The underlying corneal stroma from samples was cut into small (1-2 mm^2) pieces and placed into Collagenase Type II solution (0.006 g/mL Collagenase Type II, (Worthington Industries) 1:100 DNAse (Worthington Industries), and incubated at 37°C on a rotator for 4 hours. Cells from the epithelium, stroma and media were washed with DPBS (Lonza) and passed through a 70 µm cell strainer into 5 mL Falcon round-bottom polystyrene FACS tubes. The collected solution was centrifuged twice at 400 xg RPMI for 5 minutes and the supernatant was removed. Cells were resuspended in DPBS and labelled for flow cytometric phenotyping of surface expression markers.

Flow cytometry method. Cells were labelled and nonviable cells were excluded by staining with Fixable Viability Stain 700 (BD Bioscience), 1:5000 for 30 min on ice. Cells were blocked for 10 minutes on ice with 5% human AB serum (Sigma-Aldrich). Antibody cocktail was added in Brilliant Stain Buffer (BD Bioscience), then incubated on ice for 30 mins, washed twice by adding 2 mL FACSwash (PBS with 1% FBS (Sigma-Aldrich), 2mM EDTA (Sigma-Aldrich), 0.1% Sodium Azide (Sigma-Aldrich), then centrifuging at 400 xg for 5 mins, and discarding supernatant. Cells were fixed in Cytofix (BD Biosciences) for 15 minutes at room temperature, then washed with FACS wash, as above. Flow cytometry was performed using BD Symphony and data were analysed by FlowJo. Flow cytometry antibodies included from BD were: CD45 BUV805 (HI30), HLA-DR BUV395 (G46-6) CD14 BUV737 (M5E2), CD3 BUV496 (UCHT1), from Biolegend was: CD19 BV750 (HIB19), from Miltenyi Biotec CD1c PE (AD5-8E7), Langerin PE Vio770 (MB22-9F5).

Intravital imaging of GFP+ T cells in mouse corneas: Mice were anaesthetized with isoflurane (3.0% induction, maintained at 1.5%, vaporised in a mixture of 80:20 oxygen and air). Mice were placed in a head holder (Narashige) and the imaged eye was anaesthetized using one drop of topical anesthetic (Alcaine 0.5%, Alcon, USA) for five minutes. The eye was gently exposed from the socket and secured using a plastic loop, a cone placed around the eye, sealed with vacuum grease, and filled with PBS. Intravital imaging was performed in a custom-made environmental chamber (Precision Plastics) maintained at 35°C using heated air. Image acquisition was performed with a Zeiss LSM710 NLO multi-photon microscope (Carl Zeiss Microimaging) using a 20X/1.0 NA water immersion objective. The tissue was excited at 925 nm using a two-photon Ti:sapphire femto-second pulsed laser (Chameleon Vision II, Coherent Scientific). Three dimensional stacks were acquired at 30–40 second intervals for 30–40 minutes. Data and movies were processed using Imaris 8.3.1 (Bitplane).

Ex vivo mouse IVCM imaging and immunostaining. Immediately after euthanasia, eyes were fixed in 1% paraformaldehyde for 1 minute and imaged immediately with the Heidelberg Retina Tomograph 3 (HRT-3) with Rostock Corneal Module (Heidelberg Engineering GMB, Germany, Fig. 1A). The mouse eye was oriented manually, and volume (Z-stack) scans were taken of the entire corneal thickness at the paracentral cornea. Eyes were lubricated using Genteal Gel (Alcon, USA), and after imaging was completed, eyes were post-fixed and processed for immunofluorescence staining.

Immunostaining. Excised mouse corneas were fixed in 4% paraformaldehyde for up to 1 hour. Following permeabilization with 25mM ethylenediaminetetraacetic acid for 1 hour at 37°C, the corneas were blocked with a buffer of 3% BSA and 0.3% Triton-X for 1 hour at room temperature and stained with CD45 (1:500; Cat #550539, BD Biosciences, NJ, USA) in PBS overnight at room temperature. Corneas were subsequently washed and stained with CD3-647 (1:200; Cat# 317312, Biolegend, CA, USA), Thy1.1-488 (1:500; Cat# 202506, Biolegend, CA, USA), goat anti-rat Alexa

Fluor 555 (1:500; Cat# A21434, Invitrogen, MA, USA) and Hoechst (1:1000; Cat#14533, Sigma-Aldrich, MO, USA) in PBS for at least 2 hours at room temperature. The stained samples were washed and mounted onto slides with Prolong® Gold. After drying, tile scans of the corneal basal epithelium were acquired using a Zeiss LSM 780 confocal microscope.

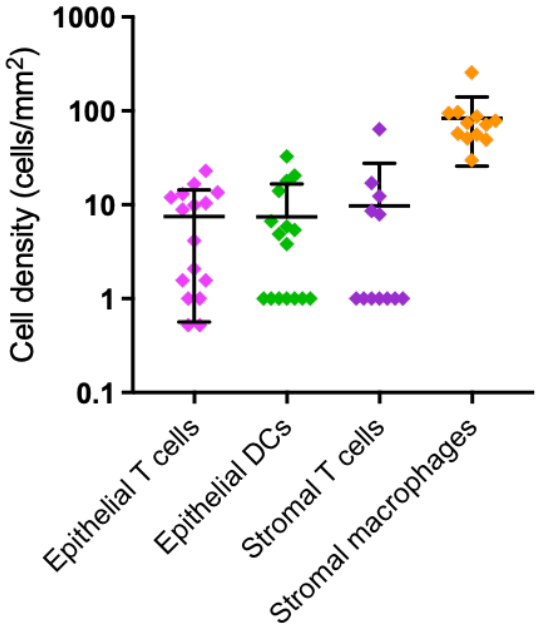

Fig. S1. Immune cell density in healthy human corneas based on Fun-IVCM imaging. Plot showing the density of corneal immune cell subtypes, stratified by corneal layer, determined from Fun-IVCM imaging of 16 healthy adult corneas. Data are summarized by the mean and standard deviation.

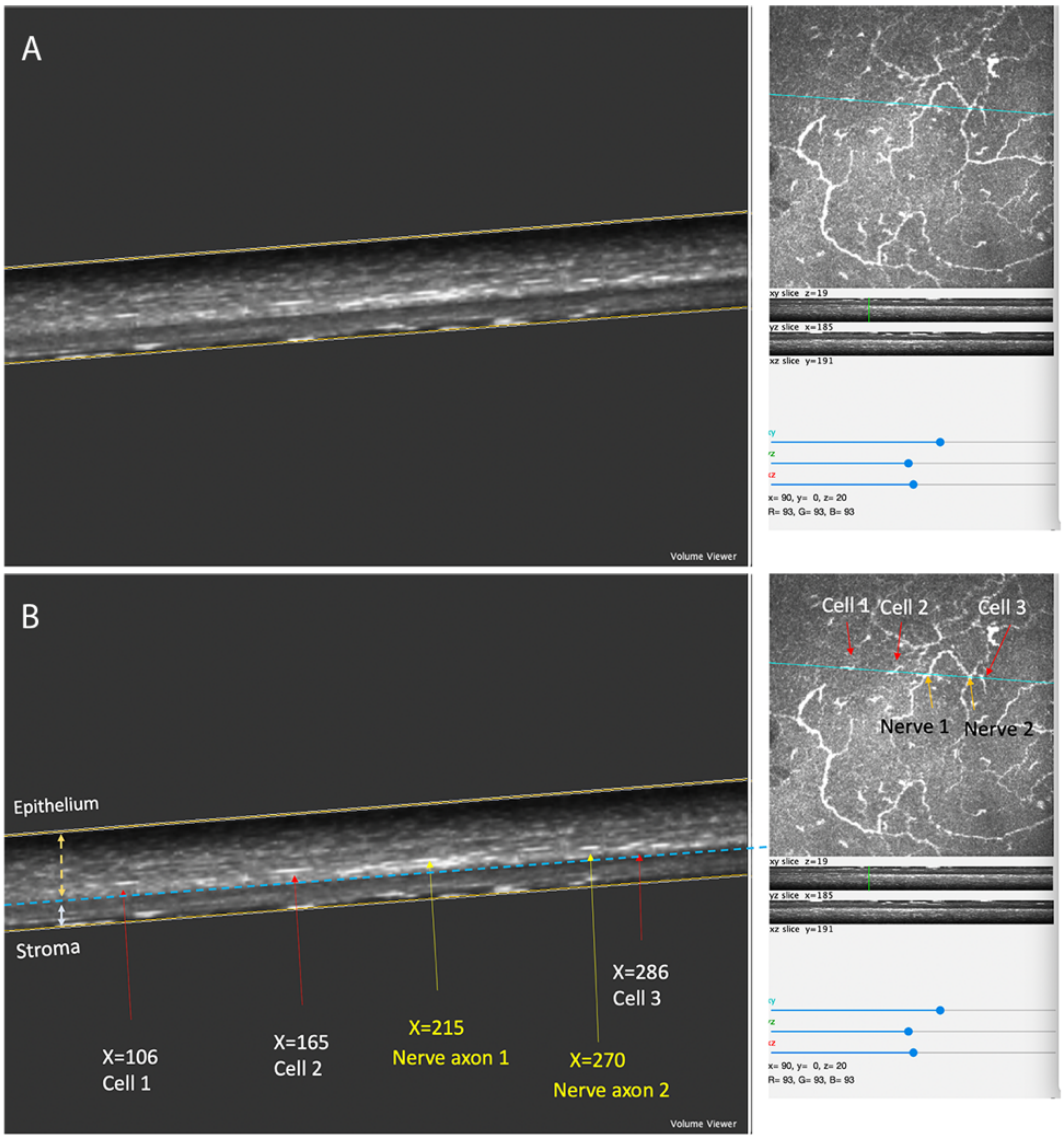

Fig. S2. Reconstructed IVCM volume scan of the healthy human cornea demonstrating the location of the nerve axons and immune cells in the same plane of focus within the sub-basal epithelial layer. (A) Original view of the Z profile of the corneal scan at the location corresponding to the cyan line in the *en face* panel. (B) Labeled images depicting three cells and two nerve axons that intersect with the cyan line, as determined by the XY coordinates.

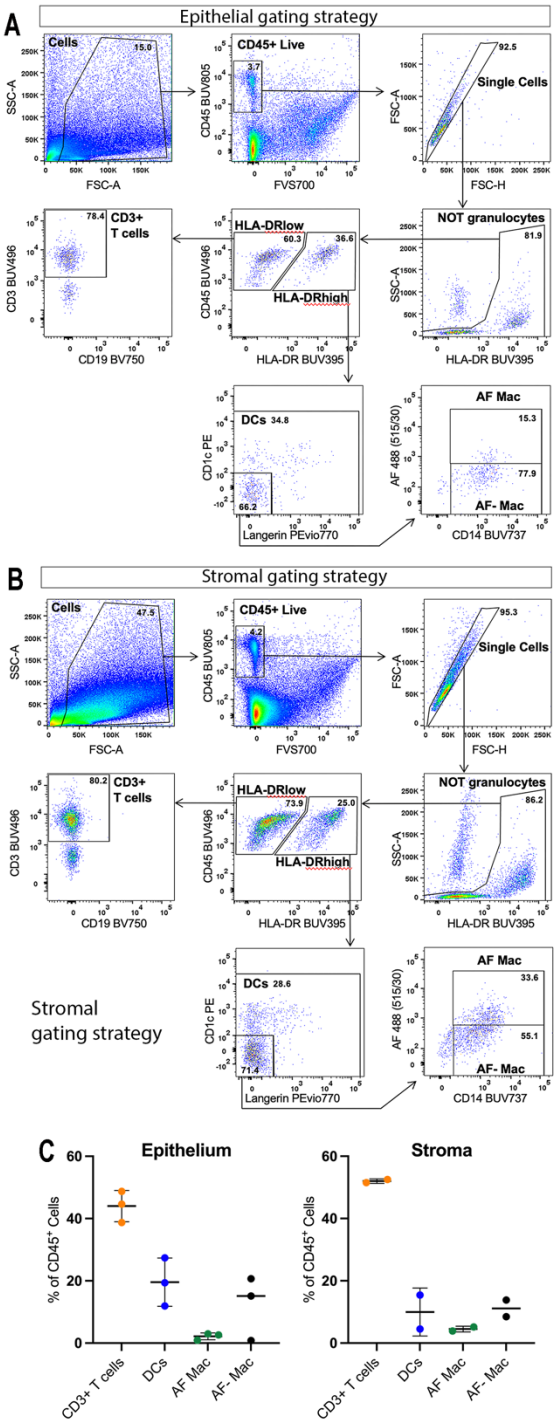

Fig. S3 Flow cytometry of human corneal immune cells. Gating strategies for CD45+ live immune cells isolated from the corneal epithelium (A) and stromal layer (B). T cells were identified as HLA-DR^{low}, CD3^{+} cells. DCs and macrophages were identified as HLA-DR^{high}, CD1c^{+} or Langerin^{+}. Macrophages were identified by CD14 expression, and further divided into autofluorescent positive and autofluorescent negative macrophage subtypes. (C) Quantitative analysis of immune cells isolated from healthy human corneal epithelium and stroma (n=3 corneas from 3 different donors).

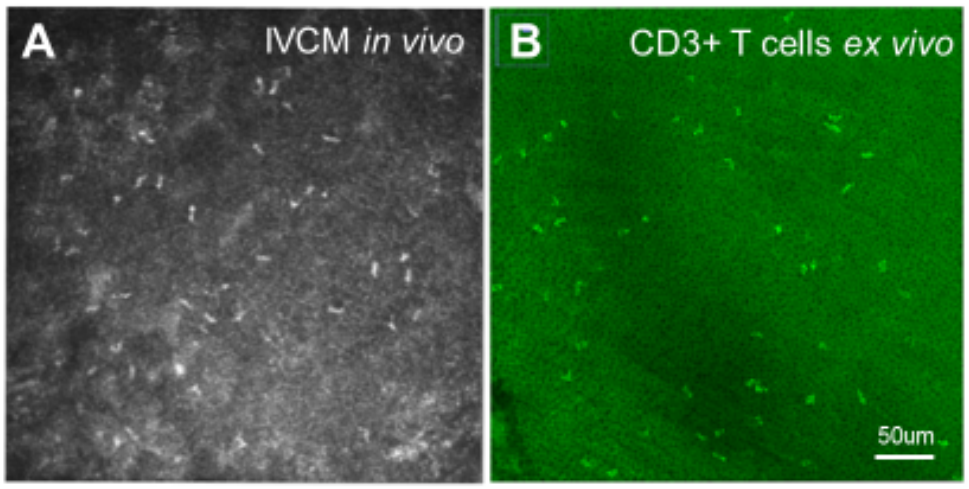

Fig. S4. Comparison of a mouse corneal IVCM image and immunohistochemical findings. (A) *In vivo* confocal microscopy (IVCM) of the cornea of a CX_3CR1-deficient mouse showing non-dendritic cell immune cells in the corneal epithelium 30 days after HSV-1 infection. (B) CD3-immunostained flatmount of the same cornea.

Table S1. *In vivo* morphological characteristics of immune cell subsets in healthy human corneas quantified from Fun-IVCM images.

	Epithelium		**Stroma**	
Parameter	**T cells** (n=65)	**DCs** (n=17)	**Macrophages** (n=26)	**T cells** (n=4)
Field area (μm^2)	81.6 ± 47.2	1171.2 ± 316.7	478.3 ± 199.2	184.2 ± 84.2
Cell area (μm^2)	55.6 ± 23.6	198.4 ± 52.4	278.6 ± 60.7	111.4 ± 8.4
Perimeter (μm)	41.4 ± 14.4	221.0 ± 88.9	100.0 ± 24.1	55.76 ± 5.8
Circularity	0.44 ± 0.13	0.04 ± 0.02	0.39 ± 0.12	0.48 ± 0.11
Roundness	0.43 ± 0.13	0.50 ± 0.23	0.45 ± 0.17	0.44 ± 0.15
Solidity	0.73 ± 0.12	0.19 ± 0.07	0.68 ± 0.10	0.76 ± 0.06

Data are shown as mean ± SD.

Table S2. Key participant characteristics

	Healthy controls (n=16)	**Untreated allergy (n=10)**	**Treated allergy (n=4)**
Age, years	29.7 ± 5.6 [range: 22 to 39]	33.2 ± 6.7 [range: 18 to 40]	35.6 ± 5.0 [range: 29 to 40]
Sex (M:F)	6:10	7:3	2:2

Table S3. Human corneal immune cell parameters quantified from Fun-IVCM time-lapsed videos

Cell feature	Category	Specific immune cell feature(s)
Static cell features(58)	*Frequency* *Morphology*	• Density (cells/mm^2). • Field area (μm^2, total area encompassed by the polygon defined by the outermost aspects of the dendrites of the cell); • Cell area (μm^2, total area encompassed by manual freehand trace around the cell border) • Perimeter (μm, distance around the edges of the cell, as determined by tracing around the cell border); • Circularity (4π x [field area/perimeter^2]); • Roundness (4 × field area/[π× major_axis^2]); • Solidity (area divided by convex hull area); • Dendritic complexity (dendritic tips/cell[a]).
Cell dynamics(18, 60)	*Motility and dendrite probing*	• Mean instantaneous speed (μm/min[b]); • Displacement speed (net cell displacement divided by total time[b]); • Meandering index (net displacement divided by total track length[b]); • Outreach ratio (maximum displacement divided by total track length[c]); • Arrest coefficient (percentage of time cell speed <2 μm/min[b]); • Linearity of forward progression (ratio of the displacement speed and mean instantaneous speed[b]); • dSEARCH (dendrite surveillance extension and retraction cycling habitude[a])(24).

[a]For DCs only; [b]For T cells only. Legend: min, minute

Movie S1 (separate file). Fun-IVCM time-lapsed imaging of the corneal epithelium in a healthy human, showing motile cells patrolling the tissue. Frames (n=7) were acquired approximately 6 minutes apart.

Movie S2 (separate file). Transgenic gBT-I.uGFP $CD8^+$ T cells imaged using intravital 2-photon microscopy in the corneal epithelium of live mice 32 days after ocular herpes simplex virus-1 infection.

Movie S3 (separate file). Fun-IVCM time-lapsed imaging of the corneal epithelium in a healthy human, showing DCs exhibiting dSEARCH dynamic behaviors. A small number of motile T cells are also visible. Images (n=6) were acquired approximately 5 minutes apart.

Movie S4 (separate file). Time-lapse confocal microscopy of intraepithelial CD11c-$eYFP^+$ cells in the mouse cornea. Images were acquired approximately 6-7 minutes apart over 30 minutes.

Movie S5 (separate file). Fun-IVCM time-lapsed imaging of the corneal stroma in a healthy human, showing amoeboid-shaped macrophages 'crawling'. Stationary keratocytes, which show minimal movement or morphological alterations, are visible. Images (n=4) were acquired approximately 5 minutes apart.

Movie S6 (separate file). Time-lapse confocal microscopy of $CX_3CR1^{GFP/+}$ macrophages in the mouse corneal stroma. Images were acquired approximately every 2 minutes over a 30-minute period.

Movie S7 (separate file). Fun-IVCM time-lapsed imaging of the corneal epithelium in a healthy human, showing T cells interacting with sensory nerves. Images (n=5) were acquired approximately 5 minutes apart.

Movie S8 (separate file). Fun-IVCM time-lapsed imaging showing a DC dendrite episodically interacting with a sensory nerve, and a DC and T cell transiently making contact with each other. Images (n=4) were acquired approximately 6 minutes apart over a 30-minute period.

References

1. J. S. Wolffsohn *et al.*, TFOS DEWS II Diagnostic Methodology report. *Ocul. Surf.* **15**, 539-574 (2017).

2. X. Y. Zhang, M. Wu, H. R. Chinnery, L. E. Downie, Defining an Optimal Sample Size for Corneal Epithelial Immune Cell Analysis Using in vivo Confocal Microscopy Images. *Front. Med.* **9**, 848776 (2022).

3. M. E. H. De Silva, A. C. Zhang, A. Karahalios, H. R. Chinnery, L. E. Downie, Laser scanning in vivo confocal microscopy (IVCM) for evaluating human corneal sub-basal nerve plexus parameters: protocol for a systematic review. *BMJ Open* **7**, e018646 (2017).

4. A. C. Britten-Jones *et al.*, Investigating the Neuroprotective Effect of Oral Omega-3 Fatty Acid Supplementation in Type 1 Diabetes (nPROOFS1): A Randomized Placebo-Controlled Trial. *Diabetes* **70**, 1794-1806 (2021).

5. A. Nishibu *et al.*, Behavioral responses of epidermal Langerhans cells in situ to local pathological stimuli. *J. Invest. Dermatol.* **126**, 787-796 (2006).